Secondary-electron and negative-ion emission from Al: Effect of oxygen coverage

J. C. Tucek, S. G. Walton, and R. L. Champion

Department of Physics, College of William and Mary, Williamsburg, Virginia 23187

(Received 27 November 1995; revised manuscript received 12 February 1996)

Absolute values for secondary-electron and negative-ion yields resulting from positive ions impacting an aluminum surface have been measured as a function of oxygen coverage on the surface. The experiments have been performed with positive sodium ions at collision energies below 500 eV. The dominant sputtered negative ion is observed to be O^- for the entire range of impact energies studied. The yields for electrons and O^-, as secondary species, exhibit similar and marked dependencies on impact energy and oxygen coverage of the surface. Using recently calculated potential parameters for the Al/O system, a specific model for the sputtering of O^- is presented. Additionally, a mechanism for the secondary emission of electrons involving the formation of $O(^1S)$ by the neutralization of the impacting Na^+ directly with O^- residing on the surface is proposed as the source of secondary electrons. [S0163-1829(96)07421-8]

I. INTRODUCTION

A complete understanding of secondary-electron and negative-ion emission resulting from low energy, ion-surface collisions is of fundamental interest to the field of surface physics. While the various aspects of secondary emission at high impact energies have been studied extensively,[1,2] little data is available for ultrahigh vacuum prepared metallic surfaces for impact energies below 500 eV. Previous investigations, however, clearly have distinguished the ''kinetic'' and ''potential'' emission processes of particle induced electron emission at low impact energies.[3,4] Kinetic emission requires a substantial momentum transfer to a conduction electron which is only likely to occur for impact energies in the keV range, where the velocity of the incoming particle is similar to that of a conduction electron with the Fermi energy. In a potential emission process, the neutralization of the incident positive ion via electron tunneling will release energy which may be transferred to another electron in the solid. That second electron can be emitted into the vacuum if the energy gained from neutralization is greater than twice the surface's work function.[5] While kinetic electron emission from clean metal surfaces at low collision energies is very improbable,[6–9] such is not the case for an adsorbate-covered surface where large secondary-electron emission coefficients are routinely observed.[10,11] The reason for the enhancement of emission is not known. Since all functional devices are inevitably gas covered, the effect of the adsorbate on electron and negative-ion emission is of great practical interest, and it remains an active area of inquiry.[12]

The specific purpose of these experiments is to investigate the role of the oxygen coverage on secondary-electron and negative-ion emission due to collisions of positive sodium ions (Na^+) with an aluminum (Al) surface. Na^+ was chosen in the present experiments to prevent potential emission from occurring since the ionization potential of Na (5.1 eV) is much less than twice the work function of Al (~4.2 eV). Previous studies illustrated the effect of alkali-metal coverage on the work function and secondary-electron and negative-ion emission;[10,13,14] however, in the present work, care was taken to not alter the work function appreciably

with the Na^+ beam. The effect of the change in the work function, induced by Na, is the subject of another study. In these experiments, the primary beam is incident at a fixed angle of 60° with respect to the surface normal of a polycrystaline Al ribbon. The absolute yields of secondary electrons and negative ions are determined for variable oxygen coverage of the Al ranging from none up to complete coverage. The yields are defined as the ratio of electrons or negative ions exiting the surface per incident ion. The Na^+ impact energy is varied from below the observed threshold (the minimum impact energy for the production of secondary negative products) up to 500 eV.

Ion-induced electron and negative-ion emission from surfaces play a critical role in the sheath thickness, equilibrium concentrations, and ion-energy distributions in plasmas, and these results should be relevant to many plasma based phenomena including plasma etching,[15,16] glow discharges,[17] and GEC (Gaseous Electronics Conference) reference cell experiments.[18,19] Additionally, secondary yields are important in understanding ion source performance,[20] the future development of particle detectors,[21–23] and the erosion of satellite materials in low earth orbits.[24] In the following, we present a complete description of the experimental procedure and the results for oxygen covered Al. Also, using recent calculations for the Al/O system,[25] a model specifically for O^- emission (the dominant negative-ion observed) along with a suggested mechanism for secondary-electron emission will be presented.

II. EXPERIMENTAL METHOD

The experiment is conducted in a fully bakeable ultrahigh vacuum chamber with a base pressure less than 2×10^{-10} Torr and is monitored by a residual gas analyzer and a standard ion gauge. The vacuum in the main chamber is maintained by a turbomolecular drag pump, five sputter ion pumps, and a titanium sublimation pump, with another sputter ion pump on the quadrupole mass analyzer housing. External to the chamber are a turbomolecular drag pumped differential line for the argon ion gun and a gas handling system which provides both the gas for the argon ion gun and for

J. C. TUCEK, S. G. WALTON, AND R. L. CHAMPION

oxygen to be introduced into the main chamber via a variable precision leak valve.

In the UHV chamber, the alkali-metal ion (Na^+) gun is aligned at an angle of 60° with respect to the surface normal. A Na^+ beam is produced from a thermal emission cation source, and its operation does not alter the pressure in the vacuum chamber. The ion source is made of a porous tungsten surface impregnated by an alkali metal compound which emits Na^+ ions when heated. The purity of the beam is reported to be greater than 99%, and no metastable ions should be present.[26] The Na^+ ions are focused on the Al surface with an einzel lens and a quadrupole lens. Opposite the Na^+ gun is a 0.1–5.0 keV argon ion gun providing an Ar^+ beam incident on the surface at an angle of 60° with respect to the surface normal. The Ar^+ beam, used for cleaning the surface, is fully rasterable over the entire surface area of the sample.

The sample is a 50×3 mm^2, high purity (99.995%) polycrystaline aluminum ribbon which is 0.038 mm thick. The surface mount aligns the ribbon vertically, perpendicular to the plane formed by the Na^+ and the Ar^+ beams. A circular (150 mm in diameter) screen of 93% transparent tungsten mesh, mounted vertically, lies 25 mm behind the surface. This assists in focusing the negative ions and electrons ejected from the surface into the extraction lens system. A cylindrical grid, with small apertures for the Na^+ and the Ar^+ beams, is mounted on a 64 mm diameter ring in the plane of the surface, forcing azimuthal symmetry about the horizontal extraction axis in the region in front of the surface.

The extraction lens stack consists of four lenses which collect and focus the negative ions and electrons emitted from the surface. The first lens collects about 75% of the negatively charged products, and the remaining portion passes down the extraction stack and is collected at the split lens. It is assumed that the sampled portion provides an accurate measure of the electron-ion fraction for all of the negative products collected. A small iron-core electromagnet is attached to the second lens which, when operating, produces an 80 G transverse magnetic field within the second lens, deflecting the electrons from the extracted negative products without appreciably affecting the negative-ion trajectories. The third lens, consisting of two half cylinders isolated from each other, has two modes of operation: to determine the ratio of negative ions to electrons for the sampled portion in order to calculate their absolute yields, and to direct the negative ions into the quadrupole mass analyzer. In the former mode, the collection side of this split lens is biased positively with respect to the other half to collect the negative ions and electrons. The ion yield, Y_x^-, is simply the ratio of sputtered negative ions to incident Na^+ ions. Likewise, the electron yield, Y_e^-, is the ratio of secondary electrons to incident positive ions. The total yield is merely the sum of the two: $Y_T^- = Y_x^- + Y_e^-$. In the negative-ion mass analysis mode, the two halves of the split lens are essentially at a common potential and are tuned to direct the ions into the entrance aperture of the quadrupole mass spectrometer, after which they are detected by a channel electron multiplier.

Time of flight (TOF) investigations of the sputtered negative ions can be performed by pulsing the Na^+ primary beam. The pulse width of the arriving sputtered negative ions

enables an estimation of the kinetic energy distribution of the sputtered negative ions to be made. A secondary feature of the TOF measurements is that, by varying the potential of the Al ribbon slightly, it is easy to confirm that the sputtered negative ions come exclusively from the Al surface being studied and not from any other element in the system. Additional experiments, at impact energies below the observed energetic threshold for sputtering, show that no negative secondaries are collected by the collection lenses even though elements near the surface, such as the grid, lie at potentials below the surface voltage. Furthermore, each element of the extraction system, other than the collection elements, was monitored independently to ensure that the current collected on those elements was negligible. Before each set of measurements is made, the surface is sputtered clean by rastering a 4.0 keV Ar^+ beam over the entire surface area for 3 h at a beam current of >1.0 μA. The surface cleanliness is checked at the start of each data set by measuring the total yield at an impact energy of 250 eV and confirming that $Y_T^-(250$ eV$) \leqslant 0.1\%$. This inequality provides our operational definition of ''clean.'' No other method, for example, Auger electron spectroscopy, is presently available in this experimental apparatus to check the surface cleanliness. Increasing the sputter cleaning time beyond the three hours does not lower $Y_T^-(250$ eV$)$ substantially. It should be stressed that the principal focus of these experiments is to develop an understanding of the role that oxygen coverage plays in enhancing the secondary-electron and negative-ion yields. The principal uncertainty in these experiments is associated with the exposure of the surface to a known flux of oxygen. This requires knowledge of the oxygen partial pressure, which is known only to an accuracy of $\pm 15\%$. Other uncertainties, associated with measuring the total emission current, are within 10%.

III. RESULTS

Figure 1 clearly illustrates the rather dramatic effect that oxygen coverage can have on the secondary-electron yields. In addition to the present measurements for clean and oxygenated Al surfaces, Fig. 1 shows the low impact energy portion of the secondary-electron yield of a similar experiment of Na^+ impacting a clean Au surface.[4] There is virtually no kinetic emission from these clean surfaces at low impact energies for ions such as Na^+ with low ionization potentials. In fact, for Au, $Y_e^- < 0.1\%$ for impact energies below 350 eV, and similarly, Y_e^- for Al is small, increasing to only $\sim 0.5\%$ at a 450 eV impact energy. The marked enhancement of the emission of electrons after an exposure of the Al surface to oxygen is illustrated clearly and can be attributed directly to the adsorbed oxygen. The amount of adsorbed oxygen on the surface is related its exposure to oxygen, and it is generally accepted that an exposure of 100 L (1 L=1 langmuir=10^{-6} Torr s) to polycrystalline Al corresponds to a surface coverage, Θ_S, of $0.75 < \Theta_S < 1.0$ monolayer of oxygen atoms with complete saturation occurring at ~ 300 L.[27–30] Very similar results are found for single crystal Al.[31,32] Hence the sticking coefficient for oxygen on Al is $\sim 1\%$. In what follows, we will continue to express the experimental results in terms of the Al surface exposure to oxygen as we have no independent method of determining Θ_S.
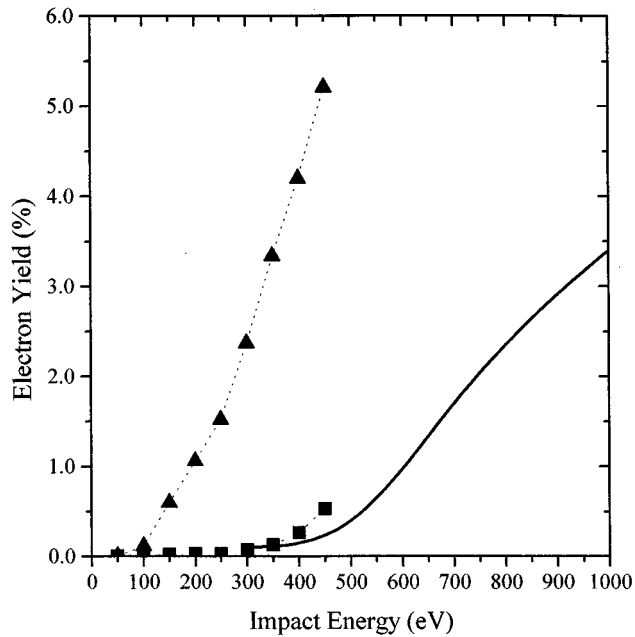
FIG. 1. Absolute electron yields for Na^+ impacting Al: ($\blacksquare$) clean and after a ($\blacktriangle$) 98 L oxygen exposure. The solid line represents the low impact energy results for Na^+ impacting clean Au and is taken from Ref. 4.

The total yield of negative products is shown in Fig. 2 as a function of impact energy for three different Al surfaces: a clean surface and two oxygen-exposed surfaces at 52 and 98 L, respectively. Y_T^- is small for a clean surface at all impact energies, and there is a considerable increase in Y_T^- with increasing surface exposure to oxygen. A doubling of the oxygen exposure almost doubles Y_T^- at a given impact energy. The energetic threshold, E_{th}, defined by linearly ex-
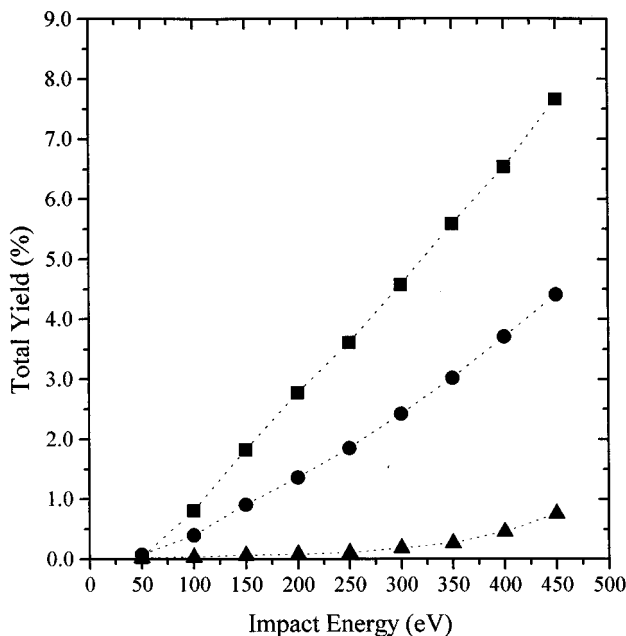

FIG. 2. Absolute yield for electrons and negative ions for Na^+ impacting Al: ($\blacktriangle$) clean, and two oxygen exposed surfaces, ($\bullet$) 52 L and ($\blacksquare$) 98 L.

trapolating the total yield curves to zero yield, is distinct at ~50 eV and independent of the aluminum's oxygen exposure. For large primary beam exposures to the surface, a significant amount of Na will adhere to the surface. This substantially alters the total yield (increasing both Y_x^- and Y_e^-), undoubtedly due to the lowering of the work function associated with alkali-metal coverage of the surface.[10,13,14] The operation of the small iron-core electromagnet, used to separate the electrons from the secondary negative ions, required that the Na^+ beam be incident on the surface at each measurement point for at least 30 s. In order to keep the Na^+ exposure of the surface to a minimum, the Na^+ current was lowered as the impact energy was increased during a set of measurements. Lowering the primary beam current did not affect Y_T^- at a given impact energy, thus ensuring that secondary emission follows from a direct, first order process, as yields are independent of the magnitude of the primary beam current striking the surface. Limiting the total Na^+ dose to the surface to <20 nA min restricts the maximum increase in Y_T^- due to the effect of Na^+ to <7% of the measured yield at the last impact energy sampled (450 eV), which would have the largest accumulated Na^+ dosage. The yield results presented in this paper have not been adjusted to compensate for this relatively small effect.

At all of the studied impact energies and oxygen exposures, the observed secondary-ion-mass spectra show that O^- is by far the dominant negative-ion species, constituting about 94% of all the sputtered negative ions with significantly smaller amounts of the molecular negative ions AlO^- (~5%) and AlO_2^- (<1%). Because of the dominance of O^-, the negative-ion yield is essentially the negative oxygen ion yield, $Y_x^- \approx Y_O^-$, and hereafter will be referred to as such. Thus the total yield can be separated into secondary-electron and O^- yields, which are shown in Fig. 3 as a function of impact energy for the previously described surfaces. While Y_O^- is small at a given impact energy for clean Al, it displays a pronounced increase with increased oxygen exposure of the Al surface. The adsorbed oxygen obviously serves as the source of O^-, whose yield begins to saturate at higher impact energies. This adsorbed oxygen also has a major effect on secondary-electron emission. Similar to Y_O^-, Y_e^- is very small for clean Al, and there is a large increase in Y_e^- with increased oxygen exposure of the Al at a given impact energy. However, as Y_O^- begins to saturate at higher impact energies, Y_e^- does not, finally surpassing Y_O^- at the highest impact energies. The increased oxygen exposure of the Al has a similar, significant effect on both Y_O^- and Y_e^-, and both share the same exposure independent threshold. These observations suggest that the yields themselves are correlated, and that the mechanism for secondary-electron emission may be coupled with the production of negative oxygen ions at low impact energies. Finally, it is of interest to note that the impact energy at which the largest relative increase in $Y_e^-(E, \Theta_s)$ is observed is at $E \approx 250$ eV for all Θ_s.

The total, electron, and negative oxygen ion yields are shown in Fig. 4 as a function of oxygen exposure of the Al surface at a fixed impact energy of 250 eV. Most importantly, a large increase in all yields is observed for increasing oxygen exposures. For exposures up to about 50 L, in addition to the observed rapid increase in the yields, there is an increase in the slopes of the yield curves. For exposures
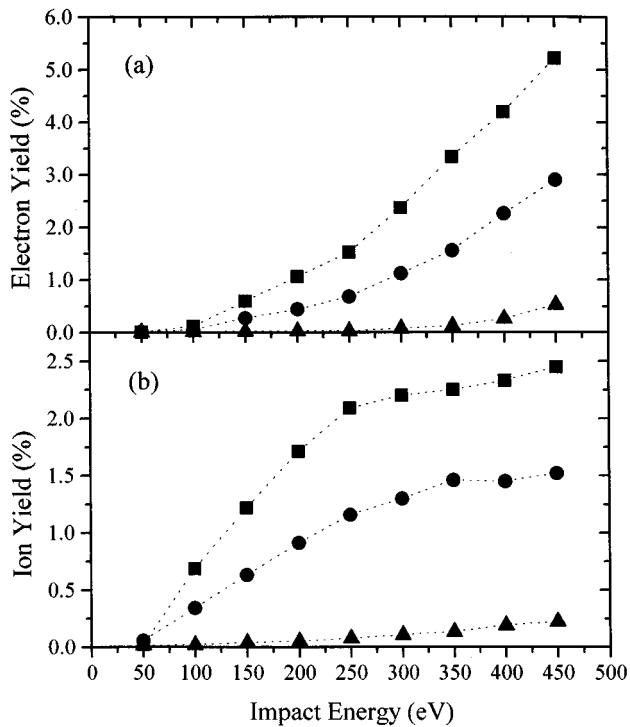
FIG. 3. (a) Absolute secondary-electron yields for Na$^+$ impacting Al: (▲) clean, and two oxygen exposed surfaces, (●) 52 L and (■) 98 L. (b) Absolute O$^-$ yields for the same three surfaces: (▲) clean, and two oxygen exposed surfaces, (●) 52 L and (■) 98 L.

ranging from 50–100 L, the yields exhibit a linear increase with exposure, and above ~100 L exposure, the slopes decrease and the yields approach saturation. These three features are possibly related to recent observations of oxygen adsorption on polycrystalline Al which show a decrease in
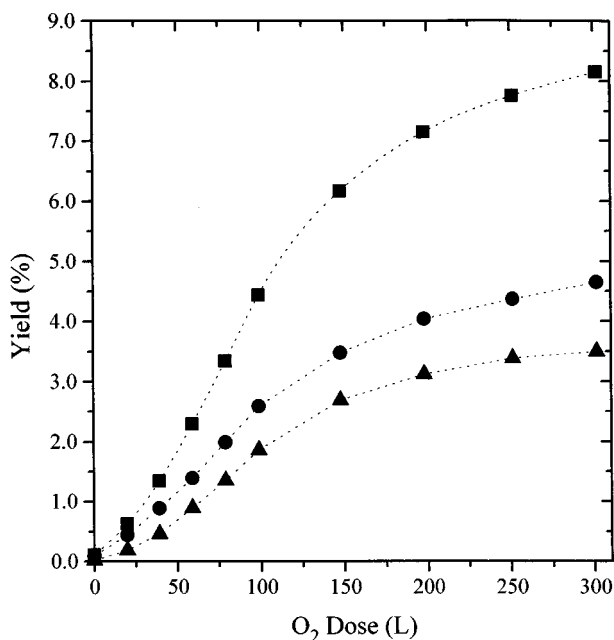

FIG. 4. Absolute (■) total, (●) O$^-$, and (▲) electron yields as a function of oxygen exposure of the Al surface at a fixed impact energy of 250 eV.

the work function, ϕ, of 0.2 eV for exposures up to ~50 L and the saturation of oxygen uptake occurring at ~100 L.[27] Thus, from 0–50 L, the increasing slope of the yield curves may be related to the obvious increase in Θ_s and the corresponding decrease in ϕ. And as the work function reaches a constant value at ~50 L, the increase of the yields becomes linear with oxygen exposure, until the saturation of the oxygen coverage of the surface occurs at ~100 L, where the yields begin to approach their saturation values.

IV. DISCUSSION

A. Secondary negative ions

Coupling of the electronic states of the metal with those of a negative ion result in a shift of the affinity level when the negative ion is sufficiently close to the metal's surface. Recent calculations specifically for the energy and width of the affinity level of O$^-$, as a function of the distance, z, from an Al surface, have been presented by Bahrim et al.[25] The shift of the affinity level was found to be very similar to that predicted by a simple image charge potential. For small distances from the reflection plane, the magnitude of the affinity level, $|E_A(z)|$, can exceed the metal's work function, ϕ. When this occurs, the O$^-$ state will lie below the Fermi level, and it is then energetically favorable for an electron from the conduction band to fill the vacancy on the oxygen atom adsorbed on the Al surface. The tunneling of an electron from the metal to the oxygen atom can occur for $z < 2.5 \ a_0$ for the Al/O system.[25] Thus oxygen adsorbed on aluminum resides on the surface essentially as a negative ion, O$^-$.

Sputtering mechanisms for the removal of surface atoms and/or ions are typically described as resulting from multiple collisions of impacting particles with atoms of the substrate, and these processes have been described extensively.[33–35] Similar mechanisms govern the sputtering of O$^-$ from an Al surface, and they may depend to some extent on the amount of oxygen on the surface. For low oxygen coverage, the impacting Na$^+$ ion will be neutralized by an electron from the metal, and the resulting Na can then sputter an O$^-$ by one of several distinct processes: (1) Na impacts an Al atom which then makes several collisions in the surface layer before ejecting an O$^-$ from the surface; (2) Na itself scatters from several Al atoms and then imparts momentum to O$^-$ ejecting it from the surface; or (3) Na impacts an O$^-$ directly which then rebounds from the surface. For higher oxygen coverage, the relative importance of (3) should increase, and the Na$^+$ is more likely to be neutralized via charge transfer directly with the O$^-$ existing on the surface. Following such a charge transfer process, an energetic oxygen atom, possibly even an excited oxygen atom, will recoil into the surface layer and then can be reflected toward the vacuum. This oxygen atom will prefer being O$^-$ again and can acquire an electron from the metal on a time scale of ~10^{-15} s which is short compared to that for exiting the surface, ~10^{-14} s.

Under any circumstances, if O$^-$ is ejected from the surface with a large enough velocity, it will survive as a negative ion independently of the exact sputtering mechanism or oxygen coverage, with the probability for survival dependent

on this exit velocity normal to the surface. The survival probability of O^- can be calculated from the fundamental rate equation,[36]

$$dP^-(t) = -\Delta[z(t)]P^-(t)dt, \qquad (1)$$

with the initial condition $P^-(t_0)=1$. Bahrim *et al.*[25] have shown that the widths, $\Delta(z)$, of the $m_l=0,\pm 1$ states of O^- can be accurately approximated by the form

$$\Delta(z) \approx \Delta_0 \exp(-\gamma z). \qquad (2)$$

The solution of Eq. (1) gives the survival probability, P_s^-, of the O^- which can be expressed as

$$P_s^-[\nu_\perp(z)] = \exp\left[-\int_{z_C}^{\infty} \frac{-\Delta(z)dz}{\nu_\perp(z)}\right], \qquad (3)$$

where $\nu_\perp(z)$ is the exit velocity of O^- normal to the surface, and z_C is the distance[37] where $|E_A(z_C)|=\phi$. With the approximation of a constant exit velocity, $\nu_\perp(z)=\nu_\perp$, the expression for P_s^- in terms of the kinetic energy, E, and the sputtering angle, θ, can be written simply as

$$P_s^-(E,\theta) \approx \exp\left[\frac{-\Delta_0 e^{-\gamma z_C}}{\gamma\sqrt{(2E/m)}\cos(\theta)}\right], \qquad (4)$$

where θ is defined as the angle at which the sputtered particles leave the surface with respect to the surface normal, and m is the mass of O^-.

In order to calculate an average survival probability with Eq. (4) the resonance width, $\Delta(z)$, for each magnetic substate and the angular and kinetic energy distribution for those O^- ions which are launched from the surface into the vacuum must be known. The magnetic substates of O^- have been shown to have rather different widths.[25] The width for the $m_l=0$ state is substantially smaller than that for $m_l=\pm 1$, which implies that the $m_l=0$ substate is the more likely substate to survive as a negative ion as it leaves the surface. An estimation of the angular and kinetic energy distribution was chosen to be of the form

$$S(E,\theta) = \left[\alpha E \exp\left(\frac{-E}{\eta U}\right) + [1-\alpha\eta^2 U^2]\frac{2UE}{(E+U)^3}\right]\cos(\theta). \qquad (5)$$

This type of distribution function has been discussed previously by others.[38] The second term is descriptive of the energy distribution based on a linear collision cascade model. The first term mimics the energy distribution associated with the sputtering after the collision cascade reaches a thermal equilibrium producing a hot spot or thermal spike from which ions can evaporate, i.e., the sputtering which occurs after most of the momentum of the impacting particle has been transferred to the lattice. The coefficient in brackets which precedes the cascade term is chosen to insure that $S(E,\theta)$ is properly normalized.

Given the launch distribution, $S(E,\theta)$, the survival distribution function is then

$$S^-(E,\theta) = S(E,\theta)P_s^-(E,\theta). \qquad (6)$$

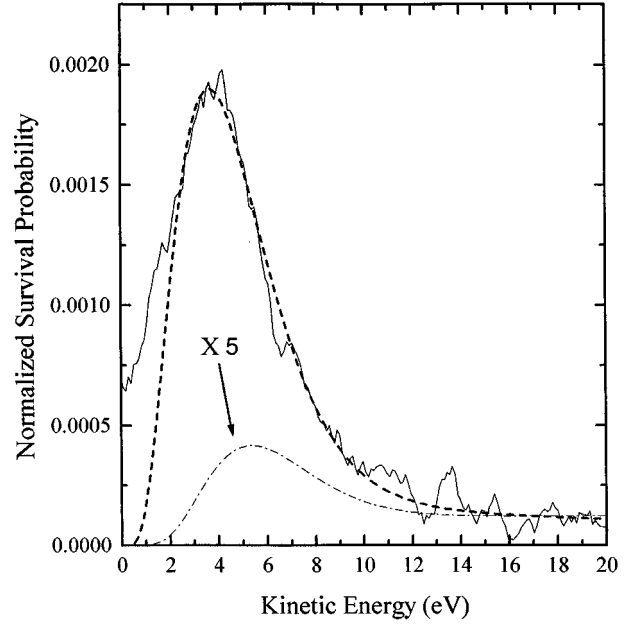Averaged over all angles (assuming azimuthal symmetry), the energy distribution becomes

FIG. 5. Sputtered O^- kinetic energy distribution for a 50 L oxygen exposed surface at an impact energy of 250 eV. The heavy, dashed (————) line is the statistical sum of the energy distributions given by Eq. (7) for the $m_l=0$, ± 1 states of O^-. The dash-dot (—·—·—·—) line represents the contribution of the $m_l=1$ state which is enhanced by a factor of 5 to illustrate its features.

$$S^-(E) = \frac{1}{2\pi}\int S^-(E,\theta)d\Omega. \qquad (7)$$

This energy distribution function for the surviving ions calculated from Eq. (7) can be compared directly to TOF data for the sputtered O^-. Such a comparison is shown in Fig. 5, where the TOF data have been converted to represent a kinetic energy distribution. The experimental results are for an impact energy of 250 eV and an oxygen dose of about 50 L. The parameters in Eq. (5) for $S(E,\theta)$ have been adjusted so as to bring the calculated $S(E,\theta)$ into rough agreement with this observed TOF distribution. The energy distribution is the statistical sum of all the m_l substate distributions with the parameters $U=2.1$ eV, $\alpha=0.6$, and $\eta=0.59$.

A few caveats concerning the ''fit'' illustrated in Fig. 5 are in order. First, there is no way for us to accurately set the zero of the kinetic energy scale. This is due to a lack of precise information about various delays associated with the optics of both the Na^+ ion beam and the sputtered O^- ions which pass through the lens system, as well as the quadrupole mass spectrometer, prior to detection. Secondly, there is clearly some time dispersion of the sputtered O^- ions owing to the fact that different sputtering angles lead to different trajectories in the extraction lens stack and beyond. We have no way to account for either of these effects at this time. Consequently, the principal information contained in the TOF data is the full width of the distribution function, which is about 5 eV. Even that should represent an upper limit to the true width of the distribution function because of the aforementioned dispersion. The distribution function, $S^-(E,\theta)$, calculated for the $m_l=\pm 1$ magnetic substates of O^- leads to a full width somewhat larger than 5 eV. How-

ever, as easily seen in Fig. 5, these magnetic substates contribute very little to the total predicted O^- flux.

Now let us turn to the issue of the average survival probability by integrating Eq. (7) over all ejection energies and assuming a statistical distribution of magnetic substates. Then the total survival probability is

$$P_{tot}^- = \frac{1}{3} \sum_{m_l = 0, \pm 1} \int_0^\infty S_{m_l}^-(E) dE. \quad (8)$$

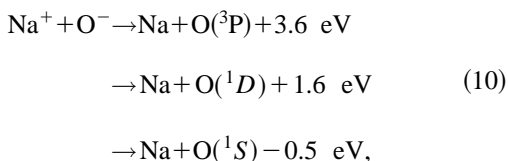We have chosen $S(E, \theta)$ to be a normalized function such that

$$2\pi \int_0^{\pi/2} \int_0^\infty S(E, \theta) \sin(\theta) dE \, d\theta = 1. \quad (9)$$

Hence P_{tot}^- will be the average probability that a sputtered O^- survives as such. The resulting value of P_{tot}^- from Eq. (8) is 1.2%. It is interesting to note that this figure is quite close to the observed O^- sputtering yield for a moderate coverage (50 L) and at a moderate collision energy (250 eV). Thus, assuming that the model provides a reasonable approximation to reality, the total sputtering yield of oxygen atoms and negative ions is predicted to be one per incident Na^+ ion for these conditions. This result is both plausible and similar to that found for other sputtering yields at comparable impact energies.[8,10,24]

B. Secondary-electron emission

Secondary-electron emission appears to be correlated to the emission of negative oxygen ions as both $Y_O^-(\Theta_s)$ and $Y_e^-(\Theta_s)$ exhibit the same energetic threshold independent of the oxygen coverage, Θ_s, and both increase similarly with increasing Θ_s at a given impact energy. While $Y_e^-(\Theta_s \approx 0)$ is very small for a clean Al surface, it significantly increases with the oxygen coverage of the surface at low impact energies. $Y_e^-(\Theta_s)$ continues to increase with impact energy, whereas $Y_O^-(\Theta_s)$ appears to approach a limiting value. As stated previously, secondary-electron emission cannot be attributed to potential or simple kinetic emission, nor can it result from an electron detaching from O^- as the ion exits the surface, since the electron would undoubtedly return to the metal due to its image charge. The similarities observed for $Y_e^-(\Theta_s)$ and $Y_O^-(\Theta_s)$ lead us to suggest another process to explain the emission of secondary electrons from Al surfaces at low impact energies.

The previously described mechanism for the neutralization of Na^+ via direct charge transfer from the O^- residing on the surface provides the most viable mechanism for the emission of a secondary electron. Charge transfer reactions for binary collisions of Na^+ with O^- can result in ground and excited state oxygen

$$Na^+ + O^- \rightarrow Na + O(^3P) + 3.6 \text{ eV}$$

$$\rightarrow Na + O(^1D) + 1.6 \text{ eV} \quad (10)$$

$$\rightarrow Na + O(^1S) - 0.5 \text{ eV},$$

where the asymptotic exothermicities are listed. An excited oxygen atom, recoiling toward the surface, can then initiate a process by which O^- is formed again and possibly ejected

into the vacuum, and at the same time, a secondary electron can be ejected. The condition for the emission of *both* an O^- and an electron from a single impacting Na^+ is that the magnitude of the affinity level, at a distance z from the surface, be at least twice the work function. For $O(^1S)$, this can occur for $z < 2.5$ a_0 since the affinity level of $O(^1S)$ lies ~4 eV below that of ground state oxygen, $O(^3P)$.[25] At $z = 2.5$ a_0, the magnitude of the affinity level of $O(^1S)$ is 8.4 eV, i.e., twice the work function of Al. The formation of O^-, by either resonant or direct transfer of a metal electron to $O(^1S)$, can provide sufficient excess energy to enable an additional electron to escape into the vacuum. For resonant transfer, an electron tunnels from the metal to the O^- vacancy, and a hole will be created in the conduction band and subsequently filled. The energy released by filling this hole can be transferred to a second electron which may be ejected into the vacuum if the deexcitation energy is greater than the work function. Similarly, the O^- vacancy can be filled directly by an electron from near the Fermi level which can release enough energy to eject another electron. With either method, both an O^- and an electron can be ejected from a single impacting Na^+. The probability that the departing O^- will survive intact en route to the vacuum is described, of course, by Eq. (8).

The cross sections for the charge transfer reactions given in (10) have not been measured. The probability for forming $O(^1S)$ should be small at low collision energies owing to the large separation between the potential energy of the products $\{Na(^2S) + O(^1S)\}$ and that for the Coulombic reactants $\{Na^+ + O^-\}$ which develops as Na^+ approaches O^-. Thus, although the asymptotic energy defect for forming $O(^1S)$ is small, the cross section for producing $O(^1S)$ will be small for low collision energies and should increase with increasing impact energy. In fact, the cross section for forming $O(^1S)$ can be anticipated to increase in a manner not unlike that observed for $Y_e^-(E)$ in the present experiments.

Evidence supporting the suggested mechanism for secondary-electron emission can be found by examining the results in Fig. 4 in a slightly different manner. The electron-O^- ratio (Y_e^-/Y_O^-, or the number of secondary electrons ejected for every O^-) is shown in Fig. 6 as a function of the oxygen exposure of the surface. For small exposures, the ratio is small, viz., ~0.2, but there is a strong dependence of the ratio on the oxygen coverage for exposures up to ~100 L as more electrons are being ejected for every O^- sputtered. As the oxygen coverage increases, the probability for forming $O(^1S)$ via charge transfer with Na^+ will increase as will the corresponding probability for secondary-electron emission. As there are several mechanisms for direct sputtering of O^- which do not involve the initial neutralization of O^- (and hence do not provide a mechanism for ejecting a secondary electron), the ratio Y_e^-/Y_O^- will be expected to increase until surface saturation is achieved for exposures in the neighborhood of 100 L. This is in fact observed to be the case.

It was mentioned earlier that the work function for Al/O decreases by about 0.2 eV for exposures of 50 L and remains constant thereafter. As discussed in Sec. II above, care was taken in the present experiments to minimize changes in the work function which will result from Na sticking to the surface. However, by exposing the surface to the Na^+ beam for
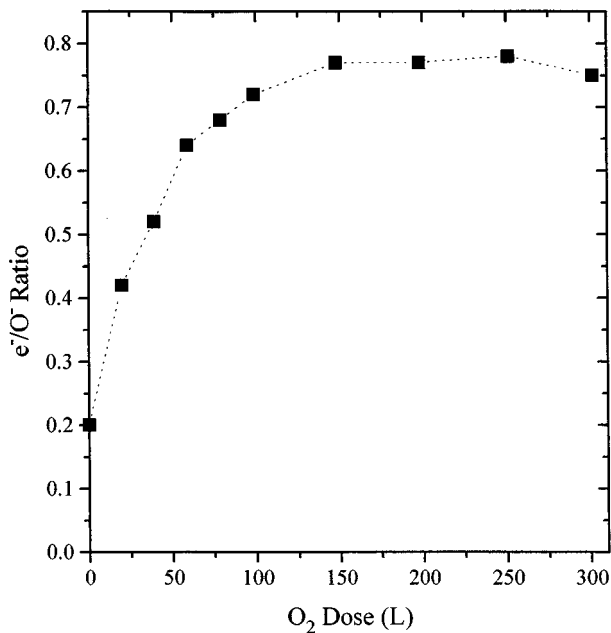
FIG. 6. Electron-O^- ratio, Y_e^-/Y_O^-, as a function of oxygen exposure of the Al surface at a fixed impact energy of 250 eV.

an extended amount of time, we can ascertain the impact of a Na-altered work function on the yields. Such measurements show that a Na-altered work function has the opposite effect on the ratio Y_e^-/Y_O^-: the ratio *decreases* as the work function decreases due to Na coverage. Hence we cannot attribute the variation observed in Fig. 6 to an oxygen-altered work function.

V. SUMMARY

The total negative-ion and secondary-electron yields for collisions of positive sodium ions with a polycrystaline alu-

minum surface at impact energies <500 eV have been measured as a function of the oxygen exposure of the surface. These yields clearly are found to be strongly dependent upon the oxygen coverage of the surface. At all the impact energies and exposures investigated, the primary negative-ion species is observed to be O^-. It has been shown that the yields exhibit a similar, marked increase with oxygen exposure at a given impact energy, and that the yields share the same, exposure-independent energetic threshold. These facts suggest that the emission of negative oxygen ions and secondary electrons is correlated. A simple model, based on calculated affinity levels and widths for O^- in front of an aluminum jellium, has been employed to describe the sputtering of O^-. This model can be adjusted to reproduce both the ion kinetic energy distribution and sputtering yield which are compatible with those observed experimentally. Additionally, a mechanism for secondary-electron emission coupled with the simultaneous sputtering of O^-, arising from a single impacting ion, has been suggested. This mechanism involves recoiling $O(^1S)$ atoms formed via the neutralization of the incoming Na^+ directly by an O^- which resides on the surface. The recoiling $O(^1S)$ atom can form O^- again in an adequately exothermic manner to simultaneously eject a conduction electron into the vacuum. The probability that this O^- is sputtered as a negative ion is dependent upon its exit velocity. Although other mechanisms might explain secondary-electron emission alone, it seems unlikely that two unrelated mechanisms, one for the desorption of O^- and another for the emission of secondary electrons, would have the same energetic threshold and a similar dependence upon oxygen coverage.

[1] *Sputtering by Particle Bombardment I*, edited by R. Behrisch (Springer-Verlag, Berlin, 1981).

[2] R. A. Baragiola, in *Low Energy Ion-Surface Interactions*, edited by J. W. Rabalais (Wiley, New York, 1993).

[3] G. Lakits, F. Aumayr, M. Heim, and H. Winter, Phys. Rev. A **42**, 5780 (1990).

[4] H. Winter, F. Aumayr, and G. Lakits, Nucl. Instrum. Methods B **58**, 301 (1991).

[5] M. Kaminsky, *Atomic and Ionic Impact Phenomena on Metal Surfaces* (Academic, New York, 1965), p. 263ff.

[6] H. Brenten, H. Müller, and V. Kempter, Surf. Sci. **271**, 103 (1992).

[7] H. Müller, R. Hausmann, H. Brenten, and V. Kempter, Surf. Sci. **291**, 78 (1993); **303**, 56 (1994).

[8] E. V. Alonso, M. A. Alurralde, and R. A. Baragiola, Surf. Sci. **166**, L155 (1986).

[9] M. Vana, F. Aumayr, P. Varga, and H. Winter, Europhys. Lett. **29**, 55 (1995).

[10] D. H. Baker, L. D. Doverspike, and R. L. Champion, Phys. Rev. A **46**, 296 (1992).

[11] W.-D. v. Fraunberg, G. Drechsler, C. Bässmann, U. Boesl, and E. W. Schlag, Int. J. Mass Spectrom. Ion Phys. **133**, 211 (1994).

[12] P. C. Smith, B. Hu, and D. N. Ruzic, J. Vac. Sci. Technol. A **12**, 2692 (1994).

[13] M. L. Yu, Phys. Rev. Lett. **40**, 574 (1978).

[14] M. Bernheim and F. Le Bourse, Nucl. Instrum. Methods B **27**, 94 (1987).

[15] E. Stoffels, W. W. Stoffels, D. Vender, M. Kando, G. M. W. Kroesen, and F. J. de Hoog, Phys. Rev. E **51**, 2425 (1995).

[16] H. You, N. M. D. Brown, and K. Al-Assadi, Surf. Sci. **284**, 263 (1993).

[17] M. Saitoh, K. Kanazawa, T. Momose, H. Ishimaru, N. Ota, and J. Uramoto, J. Vac. Sci. Technol. A **11**, 2518 (1993).

[18] P. J. Hargis *et al.*, Rev. Sci. Instrum. **65**, 140 (1994).

[19] J. K. Olthoff, R. J. Van Brunt, S. B. Radovanov, J. A. Rees, and R. Surowiec, J. Appl. Phys. **75**, 115 (1994).

[20] Z. Q. Xie and C. M. Lyneis, Rev. Sci. Instrum. **65**, 2947 (1994).

[21] G. Drechsler, C. Bässman, W.-D. v. Fraunberg, U. Boesl, and E. W. Schlag, Rev. Sci. Instrum. **65**, 3172 (1994).

[22] J. H. Arps, M. E. Miklis, and R. A. Weller, Rev. Sci. Instrum. **65**, 1575 (1994).

[23] V. Dangendorf, A. Demian, H. Friedrich, V. Wagner, A. Akkerman, A. Breskin, R. Chechik, and A. Gibrekhterman, Nucl. Instrum. Methods A **350**, 503 (1994).

[24] J. L. Allen, S. L. Espy, Y. Yao, I. F. Urazgil'din, R. G. Albridge, A. V. Barnes, and N. H. Tolk, Bull. Rus. Acad. Sci. **58**, 887 (1994).

[25] B. Bahrim, D. Teillet-Billy, and J. P. Gauyacq, Phys. Rev. B **50**, 7860 (1994); Surf. Sci. **316**, 189 (1994).

[26] Spectra-Mat Corp., Watsonville, CA.

[27] V. A. Esaulov, L. Guillemot, and S. Lacombe, Nucl. Instrum. Methods B **90**, 305 (1994).

[28] P. H. Dawson, Surf. Sci. **57**, 229 (1976).

[29] V. K. Agarwala and T. Fort, Surf. Sci. **45**, 470 (1974).

[30] W. H. Krueger and S. R. Pollack, Surf. Sci. **30**, 263 (1972).

[31] D. J. O'Connor, E. R. Wouters, A. W. Denier van der Gon, J. Vrijmoeth, P. M. Zagwijn, W. F. J. Slijkerman, J. W. M. Frenken, and J. F. van der Veen, Surf. Sci. **287/288**, 438 (1993).

[32] A. M. Bradshaw, P. Hofmann, and W. Wyrobisch, Surf. Sci. **68**, 269 (1977).

[33] Y. Yamamura, T. Takiguchi, and H. Kimura, Nucl. Instrum. Methods B **78**, 337 (1993).

[34] M. L. Yu, Nucl. Instrum. Methods B **18**, 542 (1987).

[35] W. Eckstein, C. García-Rosales, and J. Roth, Nucl. Instrum. Methods B **83**, 95 (1993).

[36] N. D. Lang and J. K. Nørskov, Phys. Scr. **T6**, 15 (1983).

[37] The values for Δ_0, γ, and z_c used in this study are inferred from the results of Ref. 25. They are $\Delta_0 = 2.414$ eV, $\gamma = 0.731a_0^{-1}$ ($m_l = 0$), and $\Delta_0 = 3.172$ eV, $\gamma = 0.630a_0^{-1}$ ($m_l = \pm 1$), with $z_c = 3.5a_0$.

[38] D. J. Oostra, R. P. van Ingen, A. Haring, A. E. de Vries, and F. W. Saris, Phys. Rev. Lett. **61**, 1392 (1988).